

Research Paper

Size-dependent Generalized Piezothermoelasticity of Microlayer

Mahdi Pakdaman¹, Yaghoub Tadi Beni^{2,3}

¹ Mechanical Engineering Department, Shahrekord University, Shahrekord, Iran

² Faculty of Engineering, Shahrekord University, Shahrekord, Iran

³ Nanotechnology Research Institute, Shahrekord, University, Shahrekord, Iran

Received March 22 2024; Revised July 02 2024; Accepted for publication July 03 2024.

Corresponding author: Y.T. Beni (tadi@eng.sku.ac.ir)

© 2024 Published by Shahid Chamran University of Ahvaz

Abstract. Nowadays, there has been a notable surge in the utilization of piezoelectric materials at the micro and nano scales, manifesting across various branches of science through the development of diverse microstructures. On the other hand, given the deployment of microstructures in environments subject to temperature fluctuations or in close proximity to heat sources, it is imperative to thoroughly examine the thermal impacts at a micro scale, particularly concerning piezoelectric materials. This paper delves into the investigation of wave propagation within a micro-scale piezoelectric layer experiencing thermal shock. This study represents the exploration of thermo-electro-elastic wave propagation within the micro dimension. For the first time, it incorporates size-dependent modeling (non-classic continuous theory) along with the application of Lord Shulman's theory to analyze the behavior of the piezoelectric layer. In the modeling process, Maxwell's three equations governing energy, motion, and electrostatics were extracted, subsequently coupled together, and finally, they were reformulated into a dimensionless form. The differential quadrature method was employed to solve the equations, and the coupled equations were resolved. Houbolt's method is employed for solving the equations in the time domain. Ultimately, the findings concerning a micro-scale piezoelectric layer under thermal shock are presented. The findings highlight the significance of size effects at the micro scale, emphasizing the necessity of considering them in analyses and applications.

Keywords: Piezothermoelasticity; generalized thermoelasticity; Lord Shulman's theory; Houbolt's method; microdomain.

1. Introduction

Classic piezoelectricity elucidates the relation between electric polarization and strain in non-centrosymmetric materials at the macro scale [1]. In recent years, the mechanical and electrical properties of piezoelectric materials have undergone scrutiny through a plethora of laboratory measurement techniques and tools. Drawing from these methodologies, researchers have observed that for piezoelectric materials at the micro and nano scales, both mechanical and electrical properties exhibit size-dependent behaviors [2-6]. Given the limitations in modeling capability associated with continuous medium theories, the development of a size-dependent theory becomes imperative. This theory should encompass the microstructure of the material by incorporating higher-order deformation gradient.

Today, there is a pronounced emphasis across various industries and fields of engineering sciences on advancing the utilization and efficiency of systems at micro and nano scales. Such systems are stimulated through various methods including thermal, electrostatic, or the utilization of smart piezoelectric materials [7]. Micro/nano systems find application across a diverse array of fields, including the manipulation of structure shapes, generation of sound waves, detection of structural defects, and extensive use in transducers, sensors, and actuators [8]. Given the capacity of piezoelectric ceramic materials to endure harsh environmental conditions, notably heat, they find versatile applications across various sectors of transportation and industries. In the design of piezoelectric microstructures, analyzing wave propagation constitutes a crucial aspect of the design process. Today, numerous microstructures employed across various engineering applications undergo thermal shock. In such instances, analyzing the thermo-electromechanical phenomena of microstructures becomes paramount [9-11].

An inherent drawback of classic coupled thermoelasticity theory is its assumption of an infinite speed for the thermal wave, stemming from the nature of the Fourier heat transfer equation. In response to this challenge and the associated physical contradiction, researchers were compelled to devise theories that simulate the speed of thermal waves with a relatively good approximation. These theories are commonly referred to as extended thermoelasticity theories [12-13]. In the simplest form, Lord and Shulman modified the conventional Fourier law by introducing a relaxation time and incorporating the rate of heat flux into the Fourier law [14]. This theory results in a restricted speed of thermal wave propagation.

Because of its simplicity and high efficiency, Lord-Shulman's theory has been widely adopted by many researchers for solving coupled thermoelasticity equations in their studies. He et al. [15] have formulated the governing equations for a piezoelectric rod



subjected to moving loading by employing Lord-Shulman's theory of thermoelasticity. In a parallel study, Babaei and Chen [16] delved into the dynamic answer of a rod that constructed with piezoelectric materials under the moving heat source, drawing upon the theory of thermoelasticity developed by Lord-Shulman. The three fully coupled dynamic differential equations were analytically solved in the Laplace domain by successively separating the equations. In the conventional Fourier's law of heat transfer, the temperature wave is assumed to propagate at an infinite speed, which poses a physical contradiction. To address this issue, various non-classic theories have been proposed. These theories are commonly referred to as extended thermoelasticity theory or thermoelasticity with the second acoustic effect. When formulated within the framework of such theories, the temperature wave propagates with a finite velocity. Kiani and Taghizadeh [17] have studied the behavior of a one-dimensional rod with piezoelectric materials using Lord-Shulman's model. To achieve this, Maxwell's three coupled equations of motion, energy and electrostatics in accordance with the three variables of mechanical displacement, electric potential, and temperature have been derived. Subsequently, these equations are developed using the differential quadrature method and tracked in the time domain. Alihemmati and Tadi Beni [18] developed the Green-Lindsay (GL) thermoelasticity theory for micro continuum bodies. They used the nonclassical modified strain gradient theory based on the Green-Lindsay theory of the micro continuum media.

Chandrasekhariah [19] has presented a theory of thermoelasticity for piezoelectric materials, encompassing heat flow among the constituent independent variables. A revised, linearized version of the theory assumes a finite velocity for thermal signals. The energy balance equation and a theorem regarding the uniqueness of solutions are presented in the aforementioned article. In a study by Zeverdejani and Kiani [20], the response of a hollow sphere made of functionally graded materials under thermal shock was investigated using the theory proposed by Lord-Shulman. Nonlinear thermal effects were taken into account in the formulation of their study. Additionally, the study involved analyzing the interaction, propagation, and reflection of waves. Heydarpour et al. [21] investigated the behavior of reinforced spherical shells under thermomechanical loading using Lord and Shulman's theory. Their proposed solution process relied on the application of the differential quadrature method, Laplace transform, and a non-uniform logical B-spline multi-stage time integration technique. Alihemmati et al. [22] developed the Chebyshev collocation numerical method for solving generalized thermoelasticity problems of the isotropic layer. The coupled thermoelastic equations are derived based on Lord-Shulman (LS), Green-Lindsay and Green-Naghdi (GN) theories.

Faraji Oskouie et al. [23] conducted a numerical study on wave propagation in a viscoelastic layer. To achieve this goal, the theory of generalized thermoelasticity (Lord-Shulman theory) was employed. Bagri and Eslami [24] formulated a one-dimensional extended thermoelastic model for discs subjected to thermal shock, drawing from Lord and Shulman's theory. The method used to solve this problem is based on the Galerkin finite element approach. Additionally, Bagheri and Eslami [25] introduced the extended coupled thermoelasticity of annular discs composed of functionally graded materials, following the theory proposed by Lord and Shulman. Kiani and Eslami [26] suggested employing the discretized differential quadrature method to solve the thermoelastic problem associated with Lord and Shulman discs. In recent years, numerous experiments conducted by researchers have demonstrated that micro-scale structures exhibit size-dependent behavior. Indeed, the mechanical properties of these structures are not only influenced by the material's type and molecular structure but also by the structure's size. Fleck et al. [27], through conducting a micro-scale twisting test on copper wires, observed that the twisting stiffness of the wires increases as the diameter of the wire decreases. Similarly, Chong and Lam [28] observed a notable size-dependent effect for epoxy beams. In their micro-bending test of polypropylene beams, McFarland and Colton [29] demonstrated a significant variance between their experimental results and those predicted by the classic theory of beams.

Certainly, piezoelectric materials are also subject to this principle. In recent years, researchers have explored the mechanical and electrical properties of piezoelectric materials through various laboratory measurement techniques and tools. Based on these methodologies, researchers have observed that for piezoelectric materials at the micro/nano scale, both mechanical and electrical properties exhibit size dependency. Consequently, high-order continuous medium theories have been employed to derive the equations governing micro/nano piezoelectric structures [30-35]. The most significant among these theories include the coupled stress theory [36-37], the strain gradient theory [38], the non-local elasticity theory [39], and the surface elasticity model [40]. Recent advancements in electromechanical micro/nano structures have introduced size-dependent theories incorporating coupled mechanical and electrical effects, such as the piezoelectric size-dependent theory. The theory of piezoelectricity in micro dimensions elucidates the relationship between electrical polarity and non-uniform strain in centrally asymmetric materials [41, 42].

Wang et al. [43] introduced a size-dependent theory based on the coupled stress theory. Considering the rotational gradient effect, they devised a formulation wherein the electric polarity was contingent upon the microscopic rotational gradient. Kheibari et al. [44] developed the Lord-Shulman generalized thermoelasticity for flexoelectric materials. The derived thermo-flexoelectricity equations showed new couplings between polarization and temperature and also between the heat conduction equation and polarization.

Throughout his research, Hadjesfandiari [45] has formulated a compatible theory for size-dependent piezoelectricity in dielectric solids. This theory demonstrates that, unlike previous flexoelectric theories which disregarded potential stress couples, electric polarization can arise due to the coupling of average curvature tensors. In this research, he has emphasized that recent advancements in micromechanics, nanomechanics, and nanotechnology necessitate sophisticated size-dependent electromechanical modeling of coupled phenomena, such as piezoelectricity.

Beni [46] analyzed piezoelectric nanobeams incorporating electromechanical coupling. In this paper, he endeavored, for the first time, to establish a nonlinear size-dependent formulation of Timoshenko's piezoelectric nanobeam in the general mode, employing the compatible coupled stress theory. The results of free vibrations indicate that the first natural vibration frequency escalates with the augmentation of the size parameter, and the outcomes of the nonlinear mode surpass those of the linear mode.

In another study, Beni [47] investigated bending, buckling, and electromechanical free vibration of functionally graded piezoelectric nanobeams, considering size dependency. In this paper, a size-dependent nonlinear formula for the functionally graded piezoelectric nanobeam has been developed using the piezoelectric size-dependent theory and the Euler-Bernoulli relation. In general, the results demonstrate that in the piezoelectric process, the generated voltage is size-dependent and diminishes with a decrease in the flexoelectric coefficient.

Tianhu et al. [48] applied the theoretical framework developed by Lord and Shulman to address a boundary value problem concerning the one-dimensional semi-infinite piezoelectric rod under an abrupt increase in temperature. The governing partial differential equations were resolved within the Laplace transform domain through the utilization of the state space methodology inherent in modern control theory. These authors in another work [49] used the theory of Green and Lindsay to deal with a thermoelastic-piezoelectric coupled two-dimensional thermal shock problem of a thick piezoelectric plate of infinite extent by means of the hybrid Laplace transform-finite element method. Various researchers investigated the effect of temperature and micro dimensions in different structures [50-52]. In all these researches, the Fourier's law has generally been used to investigate temperature variations, and the wave effects of temperature and related models have not been used in these researches. Marin et



al. [53] examined the mixed initial-boundary value problem within the framework of the Moore-Gibson-Thompson theory in thermoelasticity for dipolar bodies. The authors analyzed the phenomenon of heat conduction accompanied by dissipation. Marin et al. [54] investigated the numerical approximations of a nonlinear hyperbolic bioheat equation under different boundary conditions relevant to the medical treatment of tumor cells. Within their investigation, they explored the thermal source components in a nonlinear hyperbolic bioheat transfer model, including factors such as the rate of blood perfusions and the generation of metabolic heat, which were empirically assessed as functions dependent on temperature. Mondal et al. [55], investigated a comprehensive resolution regarding the transmission of planar waves within the generalized piezo-thermoelastic medium in the context of the two-dimensional problem, considering various thermoelastic theories including the Lord-Shulman, dual-phase lag (DPL), and three-phase lag (TPL) theories. Othman et al. [56] used the classical dynamical coupled theory, Lord-Shulman theory and Green-Lindsay to study the influence of magnetic field on piezo-thermoelastic medium. Othman and Ahmed [57] employed two distinct thermoelasticity theories in their investigation of the deformation of a generalized piezothermoelastic rotating medium under the gravitational field. A comparison was conducted between the outcomes obtained from the coupled and Green-Lindsay theories, considering both the presence and absence of rotation and gravity. In another study [58], these authors used three different thermoelasticity theories to study the deformation of a generalized piezo-thermoelastic rotating medium under the influence of gravity and magnetic field. Also, these authors [59] investigated the propagation of plane waves in generalized piezo-thermoelastic medium under the effect of rotation.

As mentioned, classic theories are inadequate for analyzing wave propagation in layers at micro and smaller sizes. Therefore, it is imperative to employ non-classic size-dependent theories that incorporate higher-order gradient of deformation to model the problem accurately.

In scenarios where the object is subjected to thermal shock, utilizing Fourier's law of thermal conductivity can yield inaccurate results. This is because, in such cases, the temperature and its gradient are high, while the duration of thermal shock occurrence is very brief, typically in the range of picoseconds. Consequently, the Fourier conduction law will fail to accurately account for wave propagation phenomena due to the very high thermal wave propagation speed. Therefore, various theories of thermoelasticity have been proposed for the thermoelastic analysis of objects under thermal shock. Due to its simplicity and efficiency, many researchers have employed Lord and Shulman's theory in their studies. In Lord-Shulman's theory, the relaxation time is introduced into Fourier's law to incorporate the wavelike motion of temperature. In essence, both the flux and its time derivative are taken into account in the thermal conductivity equation.

Based on the research conducted on the thermal wave propagation in solid mechanics, an observation can be made that the study of wave propagation in smart materials like piezoelectric and in the microscale has not yet been explored. The current study aims to delve into the thermo-electro-elastic wave propagation within the microscale, introducing a novel aspect. This research introduces the concept of size-dependent modeling, specifically the non-classic continuous theory, for the first time. Additionally, it applies Lord Shulman's theory to examine the behavior of the piezoelectric layer.

In this study, by employing size-dependent non-classic continuous medium mechanics, wave propagation in a piezoelectric layer at the micro scale was investigated and analyzed using Lord and Shulman's theory. To achieve this, coupled thermoelectromechanical equations were derived and solved using Hobolt's method.

2. Governing Equations

2.1. Energy equation

The main concept of the Lord-Shulman theory posits that relationship between temperature gradient and heat flux can be linear, with a coefficient known as the relaxation time t_0 . The Lord-Shulman equation is expressed as follows [60]:

$$q_i + t_0 \dot{q}_i = -kT_{,i}. \quad (1)$$

In the above equation, q represents the heat flux, and k is the thermal conductivity coefficient. It is worth noting that if we set t_0 equal to zero, we retrieve the classical Fourier heat conduction equation.

In the piezoelectric materials, the structural relationship for entropy can be expressed as follows [17]:

$$\dot{S} = (3\lambda + 2\mu)\alpha\dot{\epsilon} + \frac{\rho c}{T_0}\dot{\theta} - p\frac{\partial \dot{\varphi}}{\partial x}. \quad (2)$$

In the above equation, p represents the pyroelectric coefficient, T_0 is the reference temperature, $\theta = T - T_0$ is temperature change, λ and μ are the Lamé constants, and α is the linear thermal expansion coefficient. The relationship between the heat rate and the flux passing through can be expressed as follows:

$$\begin{aligned} \dot{Q} &= -\frac{\partial q}{\partial x} \\ \dot{Q} &= T_0 \dot{S} \end{aligned} \quad (3)$$

By placing Eq. (3) and Eq. (2) into Eq. (1), the following relation is derived:

$$\left(1 + t_0 \frac{\partial}{\partial t}\right) T_0 \left\{ (3\lambda + 2\mu)\alpha\dot{\epsilon} + \frac{\rho c}{T_0}\dot{T} - p\frac{\partial \dot{\varphi}}{\partial x} \right\} = k\frac{\partial^2 T}{\partial x^2}. \quad (4)$$

By placing $\epsilon_{xx} = \partial u / \partial x$ into Eq. (4), and $\beta = (3\lambda + 2\mu)\alpha$, which is referred to as the thermoelasticity parameter, the energy equation can be rewritten as follows:

$$\rho c_\epsilon (\dot{T} + t_0 \ddot{T}) + \beta T_0 \left(\frac{\partial \dot{u}}{\partial x} + t_0 \frac{\partial \ddot{u}}{\partial x} \right) - p T_0 \left(\frac{\partial \dot{\varphi}}{\partial x} + t_0 \frac{\partial \ddot{\varphi}}{\partial x} \right) = k \frac{\partial^2 T}{\partial x^2}. \quad (5)$$

2.2. Motion equation

For micro-scale structures, the equation of motion, incorporating higher-order stress parameters, can be presented as follows [35]:



$$\frac{\partial \sigma_x}{\partial x} - \frac{\partial^2 p_x}{\partial x^2} - \frac{2}{5} \frac{\partial^2 \tau_{xxx}}{\partial x^2} + \frac{3}{5} \frac{\partial^2 \tau_{yyx}}{\partial x^2} + \frac{3}{5} \frac{\partial^2 \tau_{zzx}}{\partial x^2} = \rho \frac{\partial^2 u}{\partial t^2}. \quad (6)$$

And the higher-order parameters of stress can be expressed as follows [35]:

$$\begin{aligned} p_j &= 2\mu_0^2 \gamma_j \\ \tau_{ijk}^{(1)} &= 2\mu_1^2 \eta_{ijk}^{(1)} \\ \eta_{xxx}^{(1)} &= \frac{2}{5} \frac{\partial^2 u}{\partial x^2} \\ \eta_{yyx}^{(1)} &= \eta_{xyy}^{(1)} = \eta_{xyy}^{(1)} = -\frac{1}{5} \frac{\partial^2 u}{\partial x^2} \\ \eta_{zzx}^{(1)} &= \eta_{zxx}^{(1)} = \eta_{zxx}^{(1)} = -\frac{1}{5} \frac{\partial^2 u}{\partial x^2} \\ \gamma_x &= \frac{\partial^2 u}{\partial x^2} \\ \gamma_y &= \gamma_z = 0. \end{aligned} \quad (7)$$

Parameters l_1 and l_0 indicate the dependence of mechanical characteristics on the size effect. Now, according to the constitutive equations for a piezoelectric material in the one-dimensional state, the stress components in the electric field are expressed as follows [17]:

$$\begin{aligned} \sigma_x &= (\lambda + 2\mu) \frac{\partial u}{\partial x} - \beta T - e E_x \\ E_x &= -\frac{\partial \varphi}{\partial x}. \end{aligned} \quad (8)$$

where e is the piezoelectric constant. By taking the derivative of Eq. (8) with respect to x , we can write:

$$\frac{\partial \sigma_x}{\partial x} = (\lambda + 2\mu) \frac{\partial^2 u}{\partial x^2} - \beta \frac{\partial T}{\partial x} + e \frac{\partial^2 \varphi}{\partial x^2}. \quad (9)$$

By placing Eq. (9) and Eq. (7) into Eq. (6), the motion equation will be expressed as follows:

$$(\lambda + 2\mu) \frac{\partial^2 u}{\partial x^2} - \left(2\mu_0^2 + \frac{4}{5} \mu_1^2 \right) \frac{\partial^4 u}{\partial x^4} - \beta \frac{\partial T}{\partial x} + e \frac{\partial^2 \varphi}{\partial x^2} = \rho \frac{\partial^2 u}{\partial t^2}. \quad (10)$$

2.3. Maxwell's equation

In the one-dimensional state, Maxwell's equation can be expressed as follows [45]:

$$\frac{\partial D_x}{\partial x} = 0. \quad (11)$$

where D_x represents the electrical displacement. By utilizing the piezoelectric constitutive equation, the electrical displacement relation with strain components, electric field and temperature change are illustrated as below [17]:

$$D_x = e \varepsilon_{xx} + p T + \varepsilon E_x. \quad (12)$$

in which ε is electric constant. By placing Eq. (12) and Eq. (11) into Eq. (6), the Maxwell's equation will be expressed as follows [17]:

$$e \frac{\partial^2 u}{\partial x^2} + p \frac{\partial T}{\partial x} - \varepsilon \frac{\partial^2 \varphi}{\partial x^2} = 0. \quad (13)$$

3. Non-dimensionalization of Governing Equations

The three coupled electro-theromechanical equations, derived in the last sections, are further expressed in dimensionless form. The following relationships have been utilized for non-dimensionalizing the equations:

$$\hat{u} = \left(\frac{\lambda + 2\mu}{L\beta T_0} \right) u, \quad \hat{\varphi} = \left(\frac{e}{L\beta T_0} \right) \varphi, \quad \hat{x} = \frac{x}{L}, \quad \hat{\sigma}_{xx} = \frac{\sigma_{xx}}{\beta T_0}, \quad \hat{t} = \frac{c_1}{L} t, \quad \hat{t}_0 = \frac{c_1}{L} t_0. \quad (14)$$

The parameters introduced in the above relationships are:

$$L = \frac{k}{\rho c_1 c_1}, \quad c_1 = \sqrt{\frac{\lambda + 2\mu}{\rho}}. \quad (15)$$

where c_1 represents the elastic wave propagation speed. In accordance with the introduced parameters, Eqs. (5), (10) and (13) are rendered dimensionless as follows:

$$\frac{\partial^2 \hat{u}}{\partial \hat{x}^2} - \alpha \frac{\partial^4 \hat{u}}{\partial \hat{x}^4} - \frac{\partial \hat{T}}{\partial \hat{x}} + \frac{\partial^2 \hat{\varphi}}{\partial \hat{x}^2} = \frac{\partial^2 \hat{u}}{\partial \hat{t}^2}. \quad (16)$$



$$\left(\dot{T} + t_0 \ddot{T}\right) + \alpha_2 \left(\frac{\partial \dot{u}}{\partial x} + t_0 \frac{\partial \ddot{u}}{\partial x}\right) - \alpha_3 \left(\frac{\partial \dot{\varphi}}{\partial x} + t_0 \frac{\partial \ddot{\varphi}}{\partial x}\right) = \frac{\partial^2 T}{\partial x^2}, \quad (17)$$

$$\frac{\partial^2 u}{\partial x^2} + \alpha_4 \frac{\partial T}{\partial x} - \alpha_5 \frac{\partial^2 \varphi}{\partial x^2} = 0. \quad (18)$$

where the constants employed in the above relations are equal to:

$$\alpha_1 = \left(2\mu_0^2 + \frac{4}{5}\mu_1^2\right) \left(\frac{1}{\lambda + 2\mu}\right), \alpha_2 = \frac{\beta^2 T_0}{\rho c(\lambda + 2\mu)}, \alpha_3 = \frac{p\beta T_0}{e\rho c_\varepsilon}, \alpha_4 = \frac{p}{e} \frac{\lambda + 2\mu}{\beta}, \alpha_5 = -\frac{\varepsilon}{e^2}(\lambda + 2\mu). \quad (19)$$

Also, the dimensionless representations of axial stress and electrical displacement are expressed as follows:

$$\hat{\sigma}_x = \frac{\partial u}{\partial x} - T + \frac{\partial \varphi}{\partial x}. \quad (20)$$

$$\hat{D}_x = \frac{\partial u}{\partial x} + \alpha_4 T - \alpha_5 \frac{\partial \varphi}{\partial x}. \quad (21)$$

4. Discretizing and Solving Equations

To solve the coupled Eqs. (16), (17) and (18), the differential quadrature method (GDQ) is utilized. This procedure has previously been employed to solve the coupled generalized electro-thermoelasticity in various coordinate systems [61-63]. Shu [64] was the first one who presented this method. Shu developed a mathematical method to precisely define weighting coefficients, drawing inspiration from Quan and Chang [65]. In such a situation, increasing the number of grid points does not compromise accuracy and stability.

Therefore, to initiate the discretization process, the aforementioned dimensionless equations are discretized using the following relations:

$$\begin{aligned} \sum_{j=1}^N C_{ij}^{(2)} u_j - \alpha_1 \sum_{j=1}^N C_{ij}^{(4)} u_j - \sum_{j=1}^N C_{ij}^{(1)} T_j + \sum_{j=1}^N C_{ij}^{(2)} \varphi_j - \sum_{j=1}^N C_{ij}^{(0)} \ddot{u}_j &= 0. \\ \sum_{j=1}^N C_{ij}^{(0)} T_j + t_0 \sum_{j=1}^N C_{ij}^{(0)} \dot{T}_j + \alpha_2 \sum_{j=1}^N C_{ij}^{(1)} \dot{u}_j + \alpha_2 t_0 \sum_{j=1}^N C_{ij}^{(1)} \ddot{u}_j - \alpha_3 \sum_{j=1}^N C_{ij}^{(1)} \dot{\varphi}_j + \alpha_3 t_0 \sum_{j=1}^N C_{ij}^{(1)} \ddot{\varphi}_j - \sum_{j=1}^N C_{ij}^{(2)} T_j &= 0. \\ \sum_{j=1}^N C_{ij}^{(2)} u_j + \alpha_4 \sum_{j=1}^N C_{ij}^{(1)} T_j - \alpha_5 \sum_{j=1}^N C_{ij}^{(2)} \varphi_j &= 0. \end{aligned} \quad (22)$$

In Eqs. (22), the weight coefficients utilized in the differential quadrature method are denoted by the symbol C , with N representing the number of grid points. Additionally, the superscript inside the parentheses specifies the order of the derivative. Here, u_i , T_i , and φ_i denote the displacement, temperature difference, and electric potential, respectively, at position x_i . The distribution of points is determined using the renowned Chebyshev-Gauss-Lobatto method, which is obtained according to the following equation:

$$\hat{x}_i = \frac{a}{2} \left(1 - \cos \left(\frac{i-1}{N-1} \pi \right) \right); \quad 0 \leq \hat{x}_i \leq a; \quad i = 1, 2, 3, \dots, N \quad (23)$$

The matrix form of equations (22) can be presented as follows:

$$\begin{pmatrix} M_{uu} & M_{uT} & M_{u\varphi} \\ M_{Tu} & M_{TT} & M_{T\varphi} \\ M_{\varphi u} & M_{\varphi T} & M_{\varphi\varphi} \end{pmatrix} \begin{pmatrix} \dot{u} \\ \dot{T} \\ \dot{\varphi} \end{pmatrix} + \begin{pmatrix} C_{uu} & C_{uT} & C_{u\varphi} \\ C_{Tu} & C_{TT} & C_{T\varphi} \\ C_{\varphi u} & C_{\varphi T} & C_{\varphi\varphi} \end{pmatrix} \begin{pmatrix} \dot{u} \\ \dot{T} \\ \dot{\varphi} \end{pmatrix} + \begin{pmatrix} K_{uu} & K_{uT} & K_{u\varphi} \\ K_{Tu} & K_{TT} & K_{T\varphi} \\ K_{\varphi u} & K_{\varphi T} & K_{\varphi\varphi} \end{pmatrix} \begin{pmatrix} u \\ T \\ \varphi \end{pmatrix} = \begin{pmatrix} F_u \\ F_T \\ F_\varphi \end{pmatrix} \quad (24)$$

In the above equation, F_u , F_T and F_φ are the mechanical, thermal, and electrical loading according to the boundary conditions. The matrices elements of relation (24) are calculated as follows:

Mass matrix elements:

$$\begin{aligned} M_{ij}^{uu} &= -C_{ij}^{(0)}, M_{ij}^{uT} = 0, M_{ij}^{u\varphi} = 0, M_{ij}^{Tu} = \alpha_2 t_0 C_{ij}^{(1)}, M_{ij}^{TT} = t_0 C_{ij}^{(0)}, M_{ij}^{T\varphi} = -\alpha_3 t_0 C_{ij}^{(1)}, \\ M_{ij}^{T\varphi} &= -\alpha_3 t_0 C_{ij}^{(1)}. \end{aligned} \quad (25)$$

Damping matrix elements:

$$\begin{aligned} C_{ij}^{uu} &= 0, C_{ij}^{uT} = 0, C_{ij}^{u\varphi} = 0, C_{ij}^{Tu} = \alpha_2 C_{ij}^{(1)}, C_{ij}^{TT} = C_{ij}^{(0)}, C_{ij}^{T\varphi} = -\alpha_3 C_{ij}^{(1)}, C_{ij}^{\varphi u} = 0, \\ C_{ij}^{\varphi T} &= 0, C_{ij}^{\varphi\varphi} = 0. \end{aligned} \quad (26)$$

Stiffness matrix elements:

$$\begin{aligned} K_{ij}^{uu} &= C_{ij}^{(2)} - \alpha_1 C_{ij}^{(4)}, K_{ij}^{uT} = -C_{ij}^{(1)}, K_{ij}^{u\varphi} = C_{ij}^{(2)}, K_{ij}^{Tu} = 0, K_{ij}^{TT} = -C_{ij}^{(2)}, K_{ij}^{T\varphi} = 0, \\ K_{ij}^{\varphi u} &= C_{ij}^{(2)}, K_{ij}^{\varphi T} = \alpha_4 C_{ij}^{(1)}, K_{ij}^{\varphi\varphi} = -\alpha_5 C_{ij}^{(2)}. \end{aligned} \quad (27)$$



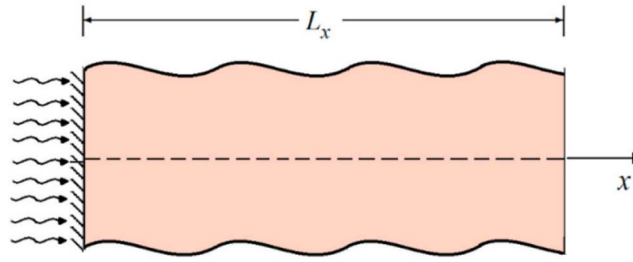


Fig. 1. Schematic of one-dimensional piezoelectric microlayer.

Furthermore, all three elements of the force vector matrix are zero.

To solve the aforementioned equations, the boundary conditions governing the problem are required. In this paper, the non-dimensionalized electro-thermomechanical boundary conditions are illustrated as follows:

$$\left\{ \begin{array}{l} \sigma_{xx} = 0 \\ \frac{\partial T}{\partial x} = 0 \\ \frac{\partial^2 u}{\partial x^2} = 0 \\ \varphi = 0 \end{array} \right. \quad x = 1 \quad ; \quad \left\{ \begin{array}{l} u = 0 \\ \frac{\partial u}{\partial x} = 0 \\ T = T_m \\ \varphi = 0 \end{array} \right. \quad x = 0 \quad (28)$$

The specified boundary conditions describe the problem such that at $x = 0$, the layer experiences thermal shock and the displacement is zero, and at $x = L$, the end of the layer is insulated and there is no stress (as depicted in Fig. (1)).

The initial conditions of the problem are assumed as follows:

$$\begin{aligned} u(x,0) &= \dot{u}(x,0) = 0 \\ T(x,0) &= \dot{T}(x,0) = 0 \\ \varphi(x,0) &= \dot{\varphi}(x,0) = 0 \end{aligned} \quad (29)$$

Several techniques exist for implementing boundary conditions on the discrete equations of motion. The boundary conditions specified in Eq. (28) are explicitly imposed on Eq. (22) in the present investigation. Subsequently, the expressions for the equations of motion and energy can be formulated. With the boundary conditions and equations governing the problem in hand, the final equations can be expressed as follows:

$$\mathbf{KX} + \mathbf{CX} + \mathbf{MX} = \mathbf{F} \quad (30)$$

The Houbolt method is employed to solve the system of time differential equations described above. To solve this system of equations, in addition to the initial values X_0 and \dot{X}_0 , the values X_1 and X_2 (corresponding to the first- and second-time steps) are required. So, to solve the equations using the Houbolt method, the values of X_1 and X_2 are initially computed through the central difference method. Subsequently, the following steps are followed for the other time steps:

$$\ddot{X}_0 = \mathbf{M}^{-1}(\mathbf{F}_0 - \mathbf{CX}_0 - \mathbf{KX}_0) \quad (31)$$

Then, by choosing the time step $\Delta t = 0.001$, the value of X_{-1} is computed as follows:

$$\ddot{X}_{-1} = \mathbf{X}_0 - \Delta t \ddot{X}_0 + \frac{\Delta t^2}{2} \ddot{X}_0 \quad (32)$$

Next, utilizing the central difference method, the values of X_1 and X_2 are determined as follows:

$$\mathbf{X}_{i+1} = \left[\frac{1}{\Delta t^2} \mathbf{M} + \frac{1}{2\Delta t} \mathbf{C} \right]^{-1} * \left\{ \mathbf{F}_i - \left(\mathbf{K} - \frac{2}{\Delta t^2} \mathbf{M} \right) \mathbf{X}_i - \left(\frac{1}{\Delta t^2} \mathbf{M} - \frac{1}{2\Delta t} \mathbf{C} \right) \mathbf{X}_{i-1} \right\}; i = 0, 1 \quad (33)$$

Now, for \mathbf{X}_{i+1} , commencing with $i = 2$, The calculation will be conducted based on the following relationship [66]:

$$\mathbf{X}_{i+1} = \left[\frac{2}{\Delta t^2} \mathbf{M} + \frac{11}{6\Delta t} \mathbf{C} + \mathbf{K} \right]^{-1} * \left\{ \mathbf{F}_{i+1} + \left(\frac{5}{\Delta t^2} \mathbf{M} + \frac{3}{\Delta t} \mathbf{C} \right) \mathbf{X}_i - \left(\frac{4}{\Delta t^2} \mathbf{M} + \frac{3}{2\Delta t} \mathbf{C} \right) \mathbf{X}_{i-2} + \left(\frac{1}{\Delta t^2} \mathbf{M} + \frac{1}{3\Delta t} \mathbf{C} \right) \mathbf{X}_{i-2} \right\} \quad (34)$$

5. Results

In the differential quadrature method, 301 nodes ($N = 301$) have been chosen. Furthermore, the dimensionless time step for solving in Houbolt's method is set to $\Delta t = 0.001$, and in the boundary conditions, the dimensionless thermal shock value applied to the beginning of the layer is taken as $\theta_m = 1$. The value of dimensionless relaxation time is also considered as $t_0 = 4$. All results are provided in dimensionless form, with the superscript $\hat{\cdot}$ omitted for ease of understanding.

Initially, to validate the derived formulas and the research solution method, we examine a scenario involving a one-dimensional piezoelectric layer subjected to temperature shock. By setting $l_1 = 0$ and l_0 in Eq. (10), we obtain the classic theory of thermoelasticity.



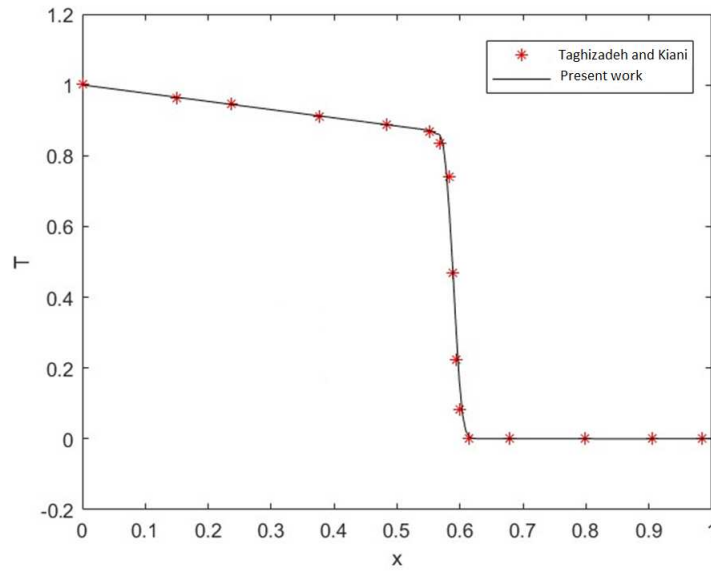


Fig. 2. The comparison of temperature graph obtained in this study with those from the research conducted by Taghizadeh and Kiani [17] at $t = 1.2$.

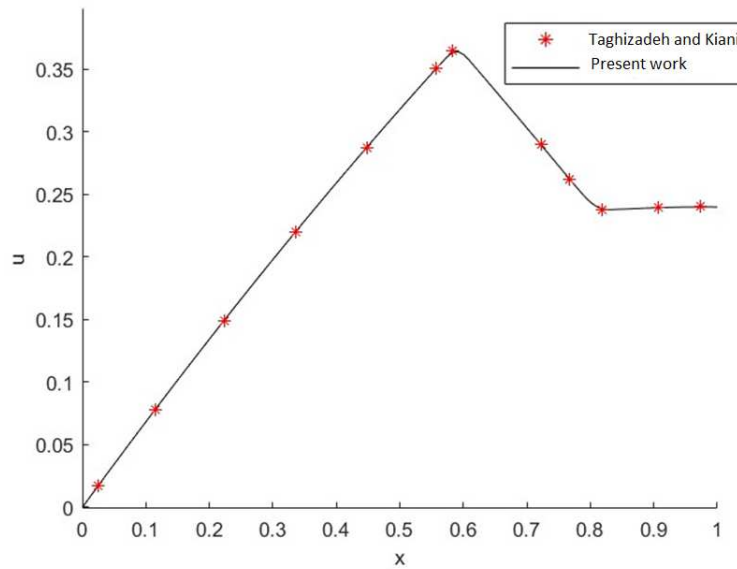


Fig. 3. The comparison of displacement obtained in this study with those from the research conducted by Taghizadeh and Kiani [17] at $t = 1.2$.

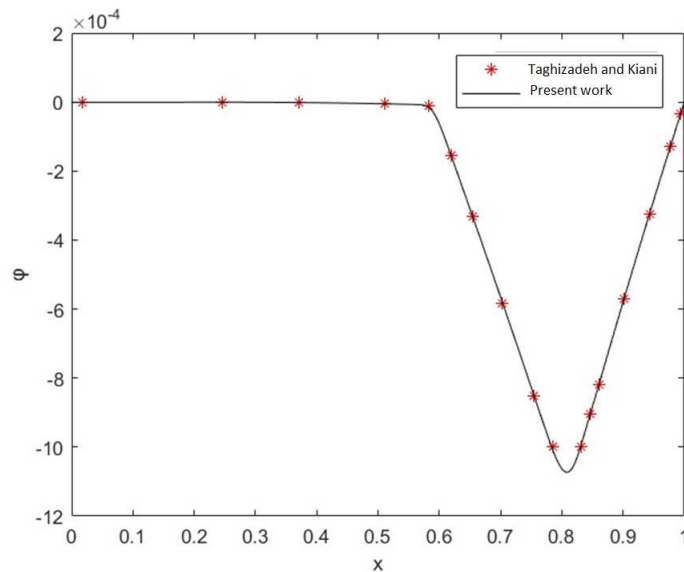


Fig. 4. The comparison of electrical potential obtained in this study with those from the research conducted by Taghizadeh and Kiani [17] at $t = 1.2$.



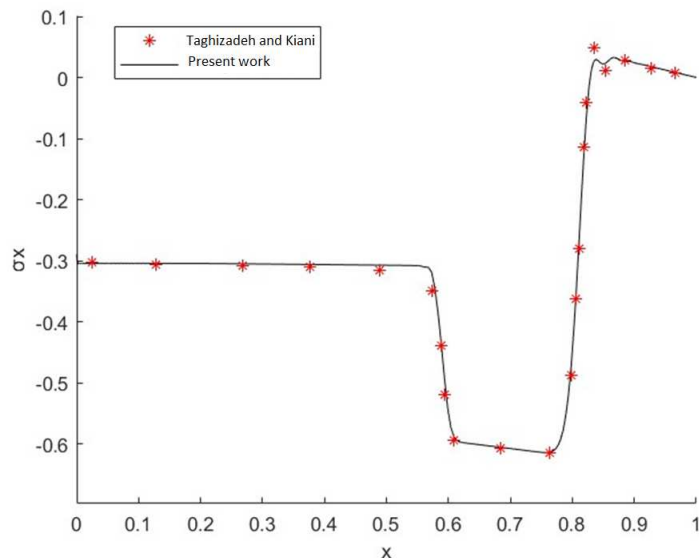


Fig. 5. The comparison of stress obtained in this study with those from the research conducted by Taghizadeh and Kiani [17] at $t = 1.2$.

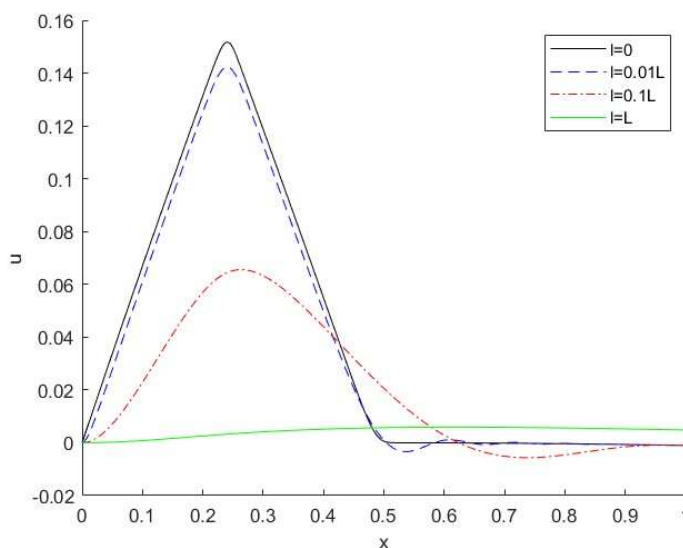


Fig. 6. Displacement distribution for the different length-scale-parameter at time $t = 0.5$.

The results obtained from this particular case have been compared with those derived from the study conducted by Kiani and Taghizadeh [17]. Figures 2 to 5 illustrate the temperature distribution and displacement. As expected, the outcomes obtained from this investigation concerning classical thermoelasticity exhibit excellent agreement with those obtained from the research conducted by Taghizadeh and Kiani [17].

Following the comparative study, a micro-scale piezoelectric layer is examined with the initial conditions outlined in Eqs. (29) and subjected to the boundary conditions described in Eq. (28). Subsequently, the coupled thermoelasticity Eq. (30) is solved. For all the figures provided herein, the used material properties are depicted in Table 1.

We assume all size effect parameters to be equal: $l_0 = l_1 = l$. Here, in order to comprehend the influence of size dependency parameters on the thermoelasticity answer of a micro-scale domain, the results for different parameter are depicted in images corresponding to different size dependency parameters. In all figures, the effects of size dependency parameters on transient thermoelastic answers are checked and explained in detail, both when the length scale is disregarded and when it is considered.

Figures 6 to 10, respectively, illustrate the displacement, temperature change, stress, electric potential, and electric displacement at dimensionless time $t = 0.5$ for various size effect parameters. As depicted in Fig. 6, the temperature change evolves gradually within the thermoelastic wavelength over a short duration. Additionally, the impact of the length scale parameters (l) on the heat dispersion shape in the non-classic state appears to be minimal. This is expected since there are no separate parameters (size effect parameters) influencing the heat transfer equation. As depicted in Fig. 7, the displacement is significantly influenced by the size effect parameter. First, in the attendance of the length scale parameter, the displacement jump of the front of elastic wave diminishes. Then, when the length scale parameters (l) become larger, the displacement decreases gradually.

Table 1. Thermoelctromechanical properties of piezoelectric material at the micro scale.

λ (GPa)	μ (GPa)	ν	ρ (kg/m ³)	β (kgK ⁻¹ m ⁻¹ s ⁻²)	C (m ² /Ks ³)	K (kgK ⁻¹ s ⁻³)	e (Cm ⁻²)	P (CK ⁻¹ m ²)	ϵ (CK ⁻¹ m ⁻²)
42.64	28.43	0.3	7820	3.34e6	4.61e2	17	0.347	-2.94	90.3e-12



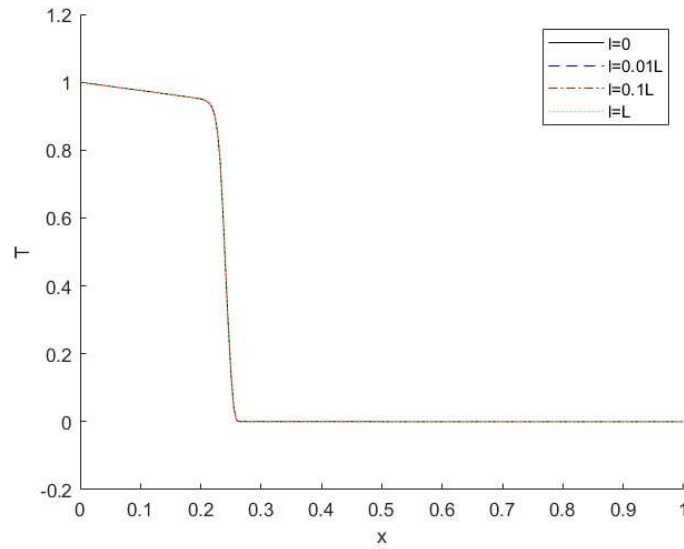


Fig. 7. Temperature distribution for the different length-scale-parameter at time $t = 0.5$.

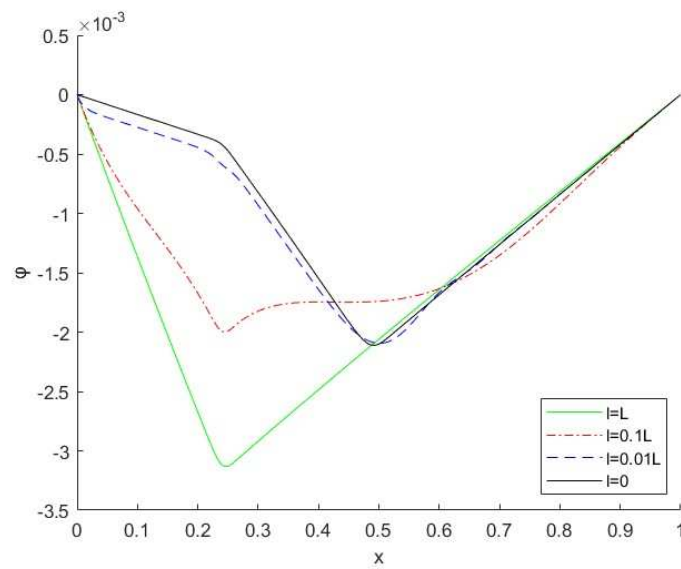


Fig. 8. Electrical potential distribution for the effect parameter of different sizes at time $t = 0.5$.

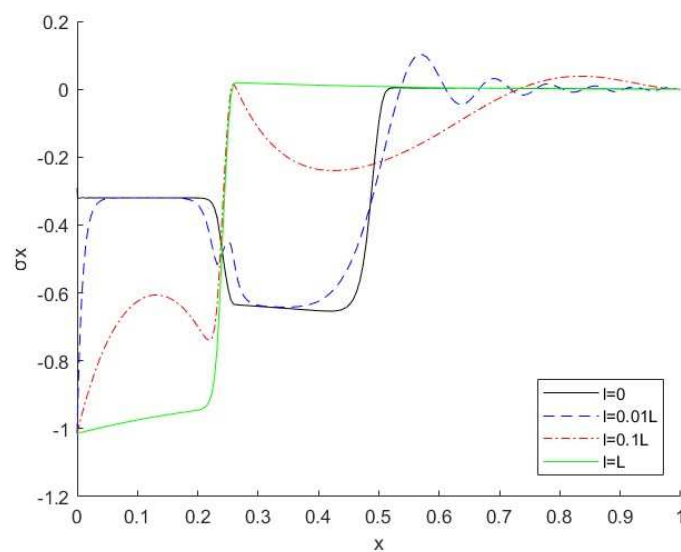


Fig. 9. Stress distribution for the different length-scale-parameter at time $t = 0.5$.



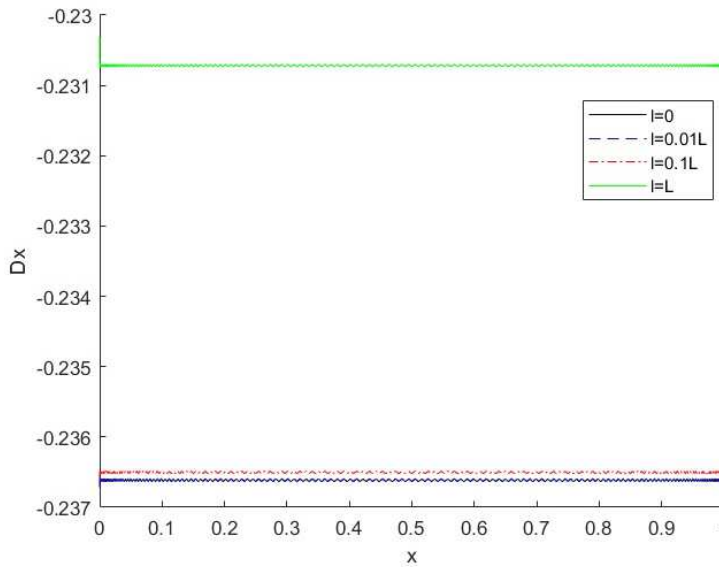


Fig. 10. Electrical displacement distribution for the different length-scale-parameter at time $t = 0.5$.

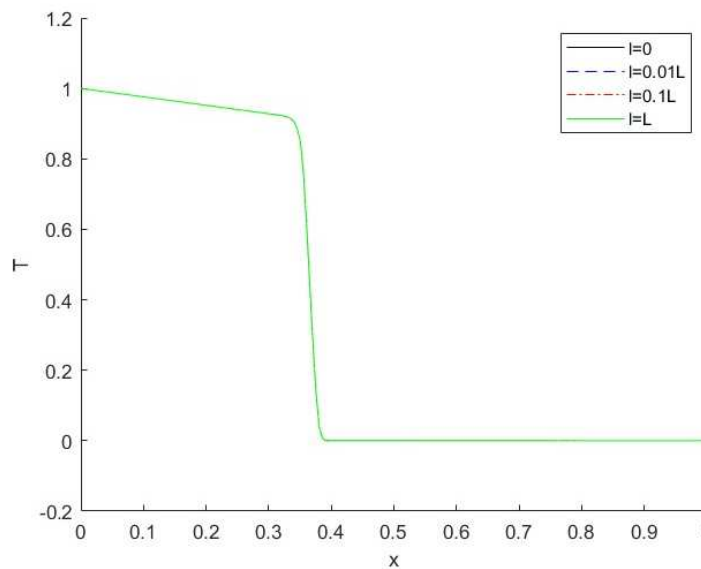


Fig. 11. Temperature distribution for the effect parameter of different sizes at time $t = 0.75$.

Moreover, Fig. 9 illustrates that the stress jump at the wave-front is eliminated when considering the length scale parameter. This aligns with higher-order continuum theories, which suggest that this nonclassical continuum model can delete the stress singularity in the wave transition. In Accordance with Eq. (18), which represents Maxwell's electrostatic equation, and as seen in Fig. 8, the electric potential wave propagation speed is infinite. Indeed, the results indicate that as soon as the temperature is applied, the entire layer will be immediately exposed to electric potential due to the coupling of the fundamental variables. It is worth noting that the two boundary conditions specifying the absence of electric potential difference at both ends are clearly evident in the results.

Figure 10 illustrates the amount of electrical displacement within the layer. The amount of displacement remains consistent across all points within the layer, aligning with what is obtained from Maxwell's equation. The propagation of this quantity exhibits a wave-like nature with infinite temperature, indicating that electrical displacement is present across the layer at all times.

Based on Eq. (17), which represents the energy equation in a dimensionless state, the velocity of wave transmission equals to $\sqrt{1/t_0}$, calculated as 0.5 in this paper. Hence, after 0.5 units of time, the front of the temperature wave will advance to 0.25, aligning with what is observed in the diagram. Analyzing the electrical potential in Fig. 7 reveals that the layer under investigation experiences the electrical potential nearly twice and with a relatively steeper slope when the size effect parameter is present.

Figures 11 through 15, respectively, display the temperature variation, displacement, electrical potential, stress, and dimensionless displacement at the time $t = 0.75$ for different size effect parameters. From the aforementioned figures, it is evident that the temperature in both classic ($l = 0$) and strain gradient (non-classic) theories, with varying size effect parameters and wave-like responses of temperature distribution in the micro-scale layer based on the modified strain gradient theory propagates with a finite velocity which can be clearly observed from Figs. 7 and 11.



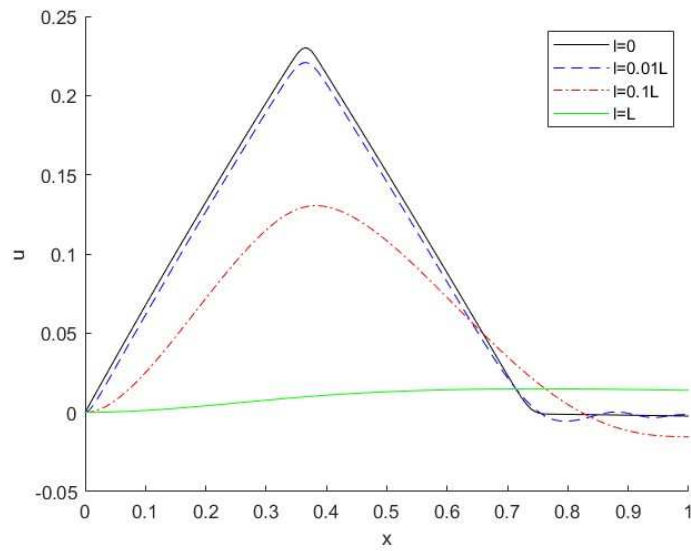


Fig. 12. Displacement distribution for the effect parameter of different sizes at time $t = 0.75$.

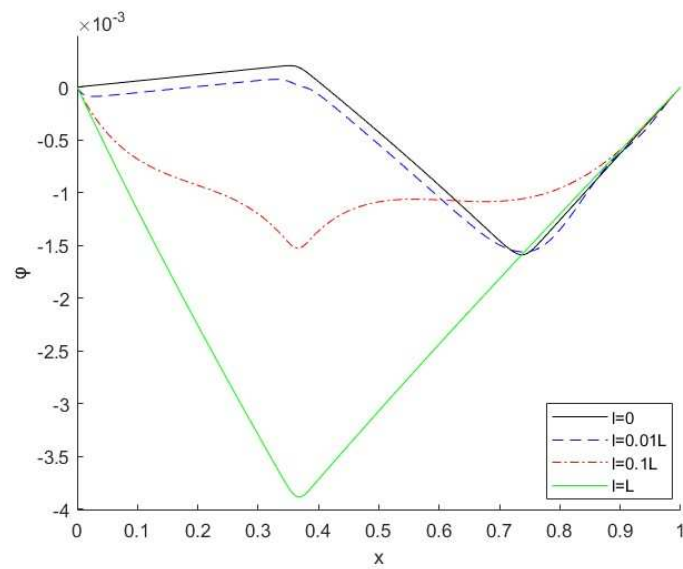


Fig. 13. Electrical potential distribution for the effect parameter of different sizes at time $t = 0.75$.

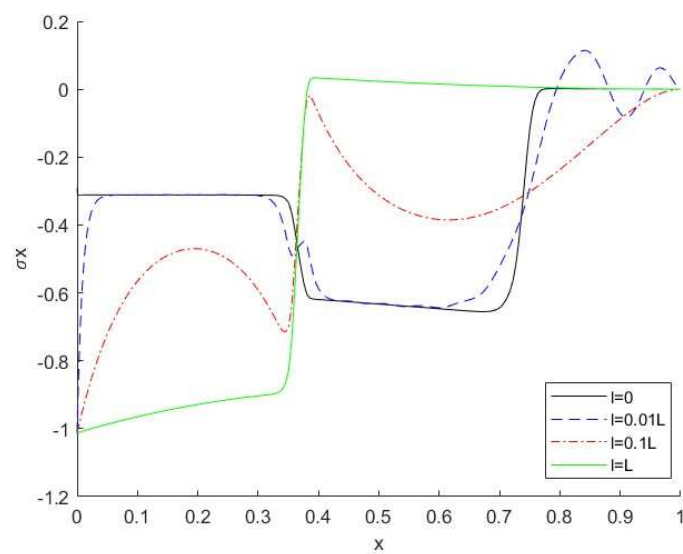


Fig. 14. Stress distribution for the different length-scale-parameter at time $t = 0.75$.



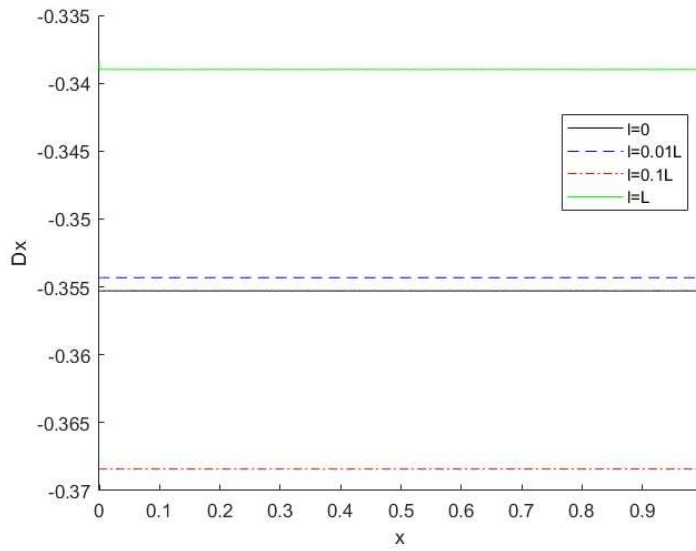


Fig. 15. Electrical displacement distribution for the different length-scale-parameter at time $t = 0.75$.

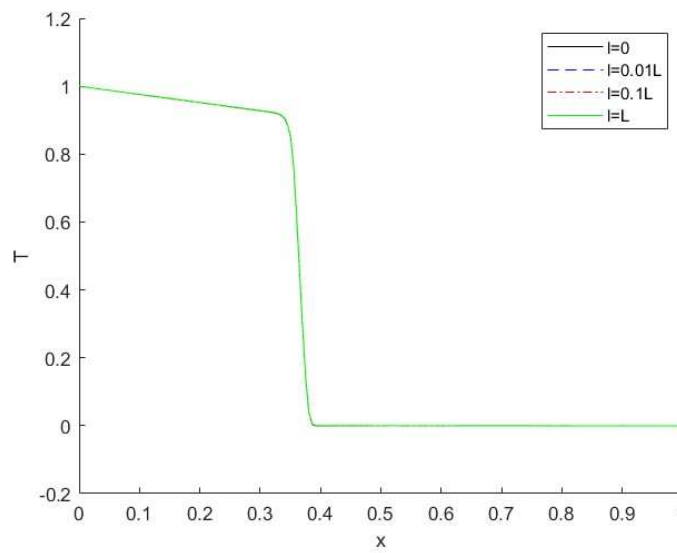


Fig. 16. Temperature distribution due to applying electrical potential for the different length-scale-parameter at time $t = 0.75$.

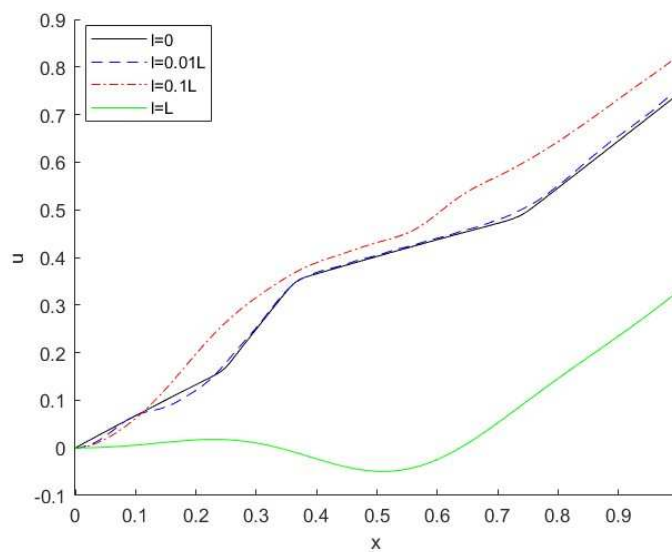


Fig. 17. Displacement distribution due to applying electrical potential for the different length-scale-parameter at time $t = 0.75$.



Figures 7 and 11 provide detailed insights indicating that the distribution of temperature under the Lord-Shulman based on the strain gradient theory exhibits a more pronounced visibility compared to the results of the classic Lord-Shulman theory for all wave propagation periods ($t = 0.5, 0.75$). The displacement distribution reveals a distinct contrast between the classical Lord-Shulman model and the modified Lord-Shulman strain gradient model. For the displacement distribution, a clear difference is observed between the classic Lord-Shulman model and the modified Lord-Shulman strain gradient model, in fact, it is obvious that only the classical Lord-Shulman results ($l = 0$) exhibit displacement wave propagation, the modified strain gradient model, according to Lord-Shulman, showcases an almost smooth distribution of displacement, with no observable wave propagation. Taking into account Eqs. (16) and (17), it becomes evident that the thermal equation resembles a wave equation along with damping, while its translational momentum equation is not as the shape of wave equation.

In the generalized thermoelasticity, stress (as per Eq. (20)) depends on displacement, temperature, and electric potential. Consequently, stress distribution is influenced and governed by these three parameters. As depicted in Figs. 9 and 14, it appears that stress distribution is predominantly influenced by temperature, exhibiting nearly wave-like responses. Since the only external load applied in this study is a thermal load, all temperature changes and resulting displacements stem from this thermal loading. According to the small pair coefficient between displacement and temperature, the values of temperatures across the entire substance range are significantly larger than the strain values. In problems involving stress loading/displacement, the stress reply differs from the current study, with displacement exerting a predominant influence on stress.

To explore the impact of applying voltage to the layer undergoing thermal shock, a dimensionless voltage value of 1 is applied at the beginning of the layer, while a dimensionless voltage of 0 is applied at the end of the layer. Figures 16 to 20 depict the diagrams of temperature variations, displacement, electrical potential, stress, and electrical displacement at dimensionless time $t = 0.75$, respectively.

Based on the results obtained, it can be concluded that applying electrical potential on piezoelectric layer does not affect temperature changes (as shown in Fig. 16). This observation is in complete agreement with the energy Eq. (18).

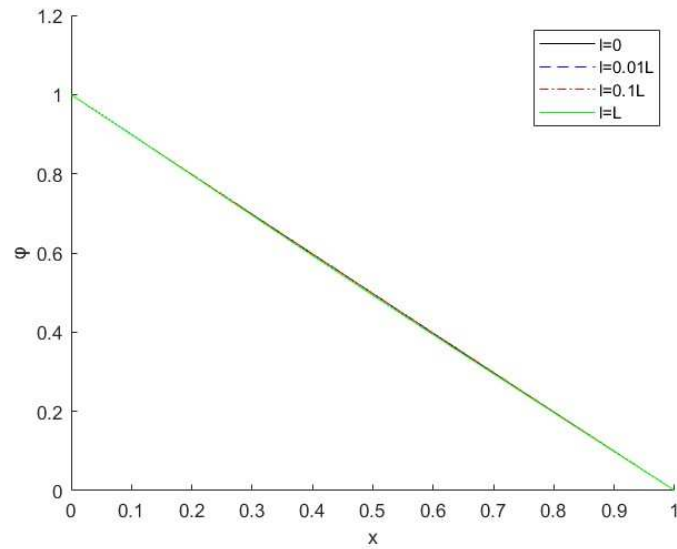


Fig. 18. Electrical potential distribution due to applying electrical potential for the different length-scale-parameter at time $t = 0.75$.

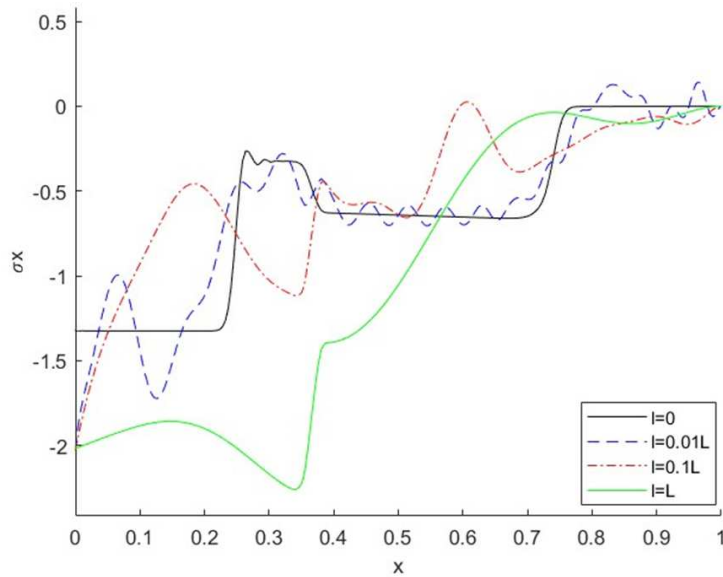


Fig. 19. Stress distribution due to applying electrical potential for the different length-scale-parameter at time $t = 0.75$.



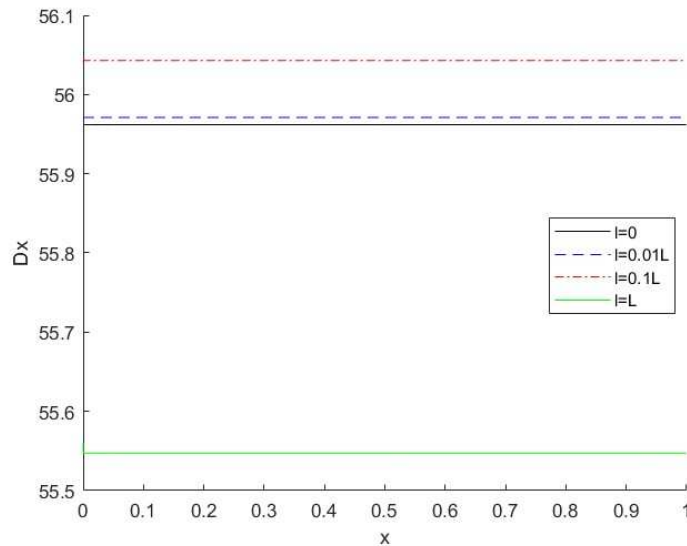


Fig. 20. Electrical displacement electrical distribution due to applying electrical potential for the different length-scale-parameter at time $t = 0.75$.

Figure 17 illustrates that the effect of the length scale parameter on the electrical potential is negligible, with the diagram in the non-classic state being nearly identical to the diagram in the classic state. This figure confirms that when a potential difference is applied, the layer experiences greater mechanical displacement compared to when only thermal shock is applied. This highlights the significance of inducing a potential difference in the piezoelectric layer and its impact on mechanical displacement.

By exploring the diagrams in Figs. 7 and 18, it can be inferred that the size effect parameter does not impact the load generator parameters (thermal shock and electrical potential difference) in the layer. Instead, its influence is observed on other coupled parameters.

6. Conclusion

In this study, the phenomenon of propagation and interference of thermo-electromechanical waves in a micro-scale piezoelectric layer were explored using Lord- Shulman's developed theory and modified strain gradient microelasticity theory. The following key findings were observed:

1. Mechanical displacement wave and temperature propagate at finite speed, while electric potential wave propagates at infinite speed.
2. The size effect parameter significantly influences the dynamic thermoelastic response of micro scale structures. Indeed, for the detailed analysis of these structures' behavior, the impact of size must be carefully considered.
3. Implementation of the size effect leads to reduced stress and displacement values, with greater reductions observed as the size effect increases.

Author Contributions

M. Pakdaman planned the scheme, initiated the project, and wrote the manuscript; Y.T. Beni examined the theory validation and offered vital direction and oversight. The manuscript was written through the contribution of all authors. All authors discussed the results, reviewed, and approved the final version of the manuscript.

Acknowledgment

Not applicable.

Conflict of Interest

The authors declared no potential conflicts of interest concerning the research, authorship, and publication of this article.

Funding

The authors received no financial support for the research, authorship, and publication of this article.

Data Availability Statements

The datasets generated and/or analyzed during the current study are available from the corresponding author on reasonable request.

References

- [1] Cady, W.G., *Piezoelectricity*, Dover Publications, Inc., New York, 1964.
- [2] Chen, C.Q., Shi, Y., Zhang, Y.S., Zhu, J., Yan, Y.J. Size dependence of Young's modulus in ZnO nanowires, *Physical Review Letters*, 96, 2006, 075505.
- [3] Xu, S.Y., Shi, Y., Kim, S.G., Fabrication and mechanical property of nano piezoelectric fibres, *Nanotechnology*, 17, 2006, 4497.




- [4] Gao, P., Liu, K., Liu, L., Wang, Z., Liao, Z., Xu, Z., Wang, W., Bai, X., Wang, E., Li, Y., Higher-order harmonic resonances and mechanical properties of individual cadmium sulphide nanowires measured by in situ transmission electron microscopy, *Journal of Electron Microscopy*, 59, 2010, 285-289.
- [5] Zhao, M.H., Wang, Z.L., Mao, S.X., Piezoelectric characterization on individual zinc oxide nanowire under piezoresponse force microscope, *Nano Letters*, 4, 2004, 587-590.
- [6] Minary-Jolandan, M., Bernal, R.A., Kuljanishvili, I., Parpoil, V., Espinosa, H.D., Individual GaN nanowires exhibit strong piezoelectricity in 3D, *Nano Letters*, 12, 2012, 970-976.
- [7] Mehralian, F., Tadi Beni, Y., Ansari, R., Size dependent buckling analysis of functionally graded piezoelectric cylindrical nanoshell, *Composite Structures*, 152, 2016, 45-61.
- [8] Quinn, P., Palacios, L., Carman, G., Speyer, J., Health monitoring of structures using directional piezoelectrics, In *Proceedings of the ASME Mechanics and Materials Conference*, Blacksburg, VA, USA, 27-30, 1999, 27-30.
- [9] Ghobadi, A., Beni, Y.T., Golestanian, H., Nonlinear thermo-electromechanical vibration analysis of size-dependent functionally graded flexoelectric nano-plate exposed magnetic field, *Archive of Applied Mechanics*, 90, 2020, 2025-2070.
- [10] Arefi, M., Abbasi, A., Vaziri Sereshk, M., Two-dimensional thermoelastic analysis of FG cylindrical shell resting on the Pasternak foundation subjected to mechanical and thermal loads based on FSDT formulation, *Journal of Thermal Stresses*, 39(5), 2016, 554-570.
- [11] Beni, Y.T., Size-Dependent Electro-Thermal Buckling Analysis of Flexoelectric Microbeams, *International Journal of Structural Stability and Dynamics*, 24(08), 2024, 2450093.
- [12] Hetnarski, R.B., Ignaczak, J., Generalized thermoelasticity, *Journal of Thermal Stresses*, 22, 1999, 451-476.
- [13] Hetnarski, R.B., Ignaczak, J., Nonclassical dynamical thermoelasticity, *International Journal of Solids and Structures*, 37(1-2), 2000, 215-224.
- [14] Lord, H.W., Shulman, Y., A generalized dynamical theory of thermoelasticity, *Journal of Mechanics of Physics and Solids*, 15, 1967, 299-309.
- [15] He, T., Cao, L., Li, S., Dynamic Response of a Piezoelectric Rod with Thermal Relaxation, *Journal of Sound and Vibration*, 306, 2007, 897-907.
- [16] Babaei, M.H., Chen, Z.T., Transient thermopiezoelectric response of a one-dimensional functionally graded piezoelectric medium to a moving heat source, *Archive of Applied Mechanics*, 80, 2010, 803-813.
- [17] Taghizadeh, A., Kiani, Y., Generalized thermoelasticity of a piezoelectric layer, *Journal of Thermal Stresses*, 42(7), 2019, 1593905.
- [18] Alihemmati, J., Tadi Beni, Y., Size dependent generalized thermoelasticity: Green-Lindsay theory with modified strain gradient theory, *Waves in Random and Complex Media*, 2022, 1-25. <https://doi.org/10.1080/17455030.2022.2105985>.
- [19] Chandrasekharaiah, D.S., A generalized linear thermoelasticity theory for piezoelectric media, *Acta Mechanica*, 71, 1988, 39-49.
- [20] Zeverdejani, P.K., Kiani, Y., Radially symmetric response of an FGM spherical pressure vessel under thermal shock using the thermally nonlinear Lord-Shulman model, *International Journal of Pressure Vessels and Piping*, 182, 2020, 104065.
- [21] Heydarpour, Y., Malekzadeh, P., Gholipour, F., Thermoelastic analysis of FG-GPLRC spherical shells under thermo-mechanical loadings based on Lord-Shulman theory, *Composites Part B: Engineering*, 164, 2019, 400-424.
- [22] Alihemmati, J., Tadi Beni, Y., Kiani, Y., Application of Chebyshev collocation method to unified generalized thermoelasticity of a finite domain, *Journal of Thermal Stresses*, 44(5), 2021, 547-565.
- [23] Oskouie, M.F., Ansari, R., Rouhi, H., Studying nonlinear thermomechanical wave propagation in a viscoelastic layer based upon the Lord-Shulman theory, *Mechanics of Advanced Materials and Structures*, 27(10), 2020, 800-806.
- [24] Bagri, A., Eslami, M., Generalized coupled thermoelasticity of disks based on the Lord-Shulman model, *Journal of Thermal Stresses*, 27(8), 2004, 691-704.
- [25] Bagri, A., Eslami, M., Generalized coupled thermoelasticity of functionally graded annular disk considering the Lord-Shulman theory, *Composite Structures*, 83(2), 2008, 168-179.
- [26] Kiani, Y., Eslami, M.R., A GDQ approach to thermally nonlinear generalized thermoelasticity of disks, *Journal of Thermal Stresses*, 40(1), 2017, 121-133.
- [27] Fleck, N.A., Muller, G.M., Ashby, M.F., Hutchinson, J.W., Strain gradient plasticity: theory and experiment, *Acta Metallurgica et Materialia*, 42, 1992, 475-487.
- [28] Chong, A., Lam, D., Strain gradient plasticity effect in indentation hardness of polymers, *Journal of Materials Research*, 14(10), 1999, 4103-10.
- [29] McFarland, A., Colton, J., Role of material microstructure in plate stiffness with relevance to microcantilever sensors, *Journal of Micromechanics and Microengineering*, 15(5), 2005, 1060-7.
- [30] Zeighampour, H., Beni, Y.T., Size-dependent vibration of fluid-conveying double-walled carbon nanotubes using couple stress shell theory, *Physica E: Low-dimensional Systems and Nanostructures*, 61, 2014, 28-39.
- [31] Zeighampour, H., Beni, Y.T., Analysis of conical shells in the framework of coupled stresses theory, *International Journal of Engineering Science*, 81, 2014, 107-122.
- [32] Zeverdejani, M.K., Beni, Y.T., Nano scale vibration of protein microtubules based on modified strain gradient theory, *Current Applied Physics*, 13(8), 2013, 1566-1576.
- [33] Balali Dehkordi, H.R., Tadi Beni, Y., Size-dependent coupled bending-torsional analysis of piezoelectric micro beams, *Mechanics Based Design of Structures and Machines*, 2023, DOI: 10.1080/15397734.2023.2278674.
- [34] Tadi Beni, Z., Tadi Beni, Y., Dynamic Stability Analysis of Size-Dependent Viscoelastic/Piezoelectric Nano-Beam, *International Journal of Structural Stability and Dynamics*, 22(05), 2022, 2250050.
- [35] Alihemmati, J., Tadi Beni, Y., Generalized thermoelasticity of microstructures: Lord-Shulman theory with modified strain gradient theory, *Mechanics of Materials*, 172, 2022, 104412.
- [36] Karimipour, I., Tadi Beni, Y., Akbarzadeh, A.H., Size-dependent nonlinear forced vibration and dynamic stability of electrically actuated micro-plates, *Communications in Nonlinear Science and Numerical Simulation*, 78, 2019, 104856.
- [37] Habibi, B., Beni, Y.T., Mehralian, F., Free vibration of magneto-electro-elastic nanobeams based on modified couple stress theory in thermal environment, *Mechanics of Advanced Materials and Structures*, 26(7), 2017, 601-613.
- [38] Tadi Beni, Y., Abadyan, M., Size-dependent pull-in instability of torsional nano-actuator, *Physica Scripta*, 88(5), 2013, 055801.
- [39] Ke, L.L., Wang, Y.S., Wang, Z.D., Nonlinear vibration of the piezoelectric nanobeams based on the nonlocal theory, *Composite Structures*, 94(6), 2012, 2038-2047.
- [40] Ansari, R., Mohammadi, V., Shojaei, M.F., Gholami, R., Sahmani, S., Postbuckling characteristics of nanobeams based on the surface elasticity theory, *Composites Part B: Engineering*, 55, 2013, 240-246.
- [41] Cady, W.G., Piezoelectricity: volume two: An Introduction to the Theory and Applications of Electromechanical Phenomena in Crystals, Courier Dover Publications, 2018.
- [42] Mishima, T., Fujioka, H., Nagakari, S., Kamigaki, K., Nambu, S., Lattice image observations of nonscale ordered in Pb(Mg₁/3Nb₂/3), *Japanese Journal of Applied Physics*, 36(9S), 1997, 6141.
- [43] Wang, G.F., Yu, S.W., Feng, X.Q., A Piezoelectric Constitutive Theory with Rotation Gradient Effects, *European Journal of Mechanics-A/Solid*, 23(3), 2004, 455-466.
- [44] Kheibari, F., Beni, Y.T., Golestanian, H., On the generalized flexothermoelasticity of a microlayer, *Acta Mechanica*, 235, 2024, 3363-3384.
- [45] Hadjesfandiari, A.R., Size-dependent piezoelectricity, *International Journal of Solids and Structures*, 50(18), 2012, 2781-2791.
- [46] Beni, Y.T., Size-dependent analysis of piezoelectric nanobeams including electro-mechanical coupling, *Mechanics Research Communications*, 75, 2016, 67-80.
- [47] Beni, Y.T., Size-dependent electromechanical bending, buckling, and free vibration analysis of functionally graded piezoelectric nanobeams, *Journal of Intelligent Material Systems and Structures*, 27(16), 2016, 2199-2215.
- [48] Tianhu H., Xiaogeng T., Shen, Y.P., State space approach to one-dimensional thermal shock problem for a semi-infinite piezoelectric rod, *International Journal of Engineering Science*, 40(10), 2002, 1081-1097.
- [49] Tianhu H., Xiaogeng T., Shen, Y.P., Two-dimensional generalized thermal shock problem of a thick piezoelectric plate of infinite extent, *International Journal of Engineering Science*, 40, 2002, 2249-2264.
- [50] Bekir, A., Civalek, Ö., Vibrational characteristics of embedded microbeams lying on a two-parameter elastic foundation in thermal environment, *Composites Part B: Engineering*, 150, 2018, 68-77.
- [51] Avcar, M., Hadji, L., Civalek, Ö., Natural frequency analysis of sigmoid functionally graded sandwich beams in the framework of high order shear deformation theory, *Composite Structures*, 276, 2021, 114564.



- [52] Khorasani, M., Soleimani-Javid, Z., Arshid, E., Lampani, L., Civalek, Ö., Thermo-elastic buckling of honeycomb micro plates integrated with FG-GNPs reinforced Epoxy skins with stretching effect, *Composite Structures*, 258, 2021, 113430.
- [53] Marin, M., Öchsner, A., Mubashir Bhatti, M., Some results in Moore-Gibson-Thompson thermoelasticity of dipolar bodies, *ZAMM-Journal of Applied Mathematics and Mechanics*, 100(12), 2021, e202000090.
- [54] Marin, M., Hobiny A., Abbas I., Finite Element Analysis of Nonlinear Bioheat Model in Skin Tissue Due to External Thermal Sources, *Mathematics*, 9(13), 2021, 1459.
- [55] Mondal, S., Othman, M.I.A., Memory dependent derivative effect on generalized piezo-thermoelastic medium under three theories, *Waves in Random and Complex Media*, 31(6), 2020, 2150–2167.
- [56] Othman, M.I.A., Elmaklizi, Y.D., Ahmed, E.A.A., Effect of magnetic field on piezo-thermo-elastic medium with three theories, *Results in Physics*, 7, 2017, 3361-3368.
- [57] Othman, M.I.A., Ahmed, E.A.A., Influence of the gravitational field on a piezothermoelastic rotating medium with G-L theory, *The European Physical Journal Plus*, 131, 2016, 358-369.
- [58] Othman, M.I.A., Ahmed, E.A.A., Exact analytical solution of a homogeneous anisotropic piezo-thermoelastic half-space of a hexagonal type under different fields with three theories, *Microsystem Technologies*, 25, 2019, 1423–1435.
- [59] Othman, M.I.A., Ahmed, E.A.A., The effect of rotation on piezo-thermoelastic medium using different theories, *Structural Engineering and Mechanics*, 56(4), 2015, 649–665.
- [60] Lord, H.W., Shulman, Y., A generalized dynamical theory of thermoelasticity, *Journal of the Mechanics and Physics of Solids*, 15, 1967, 299-309
- [61] Kiani, Y., Eslami, M.R., Nonlinear generalized thermoelasticity of an isotropic layer based on Lord-Shulman theory, *European Journal of Mechanics-A/Solid*, 61, 2017, 245–253.
- [62] Kiani, Y., Eslami, M.R., A GDQ approach to thermally nonlinear generalized thermoelasticity of disks, *Journal of Thermal Stresses*, 40(1), 2017, 121–133.
- [63] Kiani, Y., Eslami, M.R., The GDQ Approach to Thermally Nonlinear Generalized Thermoelasticity of a Hollow, *International Journal of Mechanical Sciences*, 118, 2016, 195–204.
- [64] Shu, C., *Differential Quadrature and Its Application in Engineering*, New York, Springer, 2000.
- [65] Quan, J.R., Chang, C.T., New insights in solving distributed system equations by the quadrature method –I. Analysis, *Computers and Chemical Engineering*, 13, 1989, 779–788.
- [66] Houbolt, J.C., A recurrence matrix solution for the dynamic response of elastic aircraft, *Journal of the Aeronautical Sciences*, 17, 1950, 540–550.

ORCID iD

Yaghoub Tadi Beni  <https://orcid.org/0000-0001-8565-3796>



© 2024 Shahid Chamran University of Ahvaz, Ahvaz, Iran. This article is an open access article distributed under the terms and conditions of the Creative Commons Attribution-NonCommercial 4.0 International (CC BY-NC 4.0 license) (<http://creativecommons.org/licenses/by-nc/4.0/>).

How to cite this article: Pakdaman M., Beni Y.T. Size-dependent Generalized Piezothermoelasticity of Microlayer, *J. Appl. Comput. Mech.*, xx(x), 2024, 1–16. <https://doi.org/10.22055/jacm.2024.46393.4510>

Publisher's Note Shahid Chamran University of Ahvaz remains neutral with regard to jurisdictional claims in published maps and institutional affiliations.

